Breast Cancer Research and Treatment
https://doi.org/10.1007/s10549-018-4922-8

PRECLINICAL STUDY

Fluidic shear stress increases the anti-cancer effects of ROS-generating drugs in circulating tumor cells

Sagar Regmi[1] · To Sing Fung[2] · Sierin Lim[1] · Kathy Qian Luo[2]

Received: 19 May 2018 / Accepted: 10 August 2018

Abstract

Purpose Many anti-cancer drugs are used in chemotherapy; however, little is known about their efficacy against circulating tumor cells (CTCs). In this study, we investigated whether the pulsatile fluidic shear stress (SS) in human arteries can affect the efficacy of anti-cancer drugs.

Methods Cancer cells were circulated in our microfluidic circulatory system, and their responses to drug and SS treatments were determined using various assays. Breast and cervical cancer cells that stably expressed apoptotic sensor proteins were used to determine apoptosis in real-time by fluorescence resonance energy transfer (FRET)-based imaging microscopy. The occurrence of cell death in non-sensor cells were revealed by annexin V and propidium iodide staining. Cell viability was determined by MTT assay. Intracellular reactive oxygen species (ROS) levels were determined by staining cells with two ROS-detecting dyes: 2′,7′-dichlorofluorescin diacetate and dihydroethidium.

Results Fluidic SS significantly increased the potency of the ROS-generating drugs doxorubicin (DOX) and cisplatin but had little effect on the non-ROS-generating drugs Taxol and etoposide. Co-treatment with SS and ROS-generating drugs dramatically elevated ROS levels in CTCs, while the addition of antioxidants abolished the pro-apoptotic effects of DOX and cisplatin. More importantly, the synergistic killing effects of SS and DOX or cisplatin were confirmed in circulated lung, breast, and cervical cancer cells, some of which have a strong metastatic ability.

Conclusions These findings suggest that ROS-generating drugs are more potent than non-ROS-generating drugs for destroying CTCs under pulsatile fluidic conditions present in the bloodstream. This new information is highly valuable for developing novel therapies to eradicate CTCs in the circulation and prevent metastasis.

Keywords Circulating tumor cells · Shear stress · Reactive oxygen species · Apoptosis · Anti-cancer drugs · Doxorubicin

Introduction

Despite advancements in anti-cancer drug development in recent decades, metastatic cancer remains an incurable disease that takes the lives of more than 90% of cancer patients [1, 2]. Resistance to chemotherapy is believed to be a significant problem that causes treatment failure in most metastatic cancer patients [3]. Metastasis is a multistep process in which cancer cells travel through the circulatory system to form metastatic tumors at distant sites. Thus, circulating tumor cells (CTCs) are considered to be the origin of metastasis [4]. Previously, CTCs were identified in the blood of cancer patients with solid tumors, which demonstrated the presence of CTCs in the vascular system [5, 6]. Current research on CTCs mainly focuses on detecting and diagnosing CTCs [7]. For example, several studies have shown that the number of CTCs present in the blood determines the severity of the disease [8–11]. Many oncologists consider CTCs isolated from the blood to be a "fluid biopsy" [12]. As CTCs are the cause of metastasis, more efforts should be made to develop new strategies to destroy these cells in the circulation, which will be an effective way to prevent metastasis.

To study CTCs, we have developed a microfluidic circulatory system that can generate physiological levels of fluidic shear stress (SS) similar to those present in human arteries and veins [13]. More importantly, this SS can be applied to

✉ Kathy Qian Luo
kluo@umac.mo

[1] School of Chemical and Biomedical Engineering, Nanyang Technological University, Singapore, Singapore

[2] Faculty of Health Sciences, University of Macau, Taipa, Macau, China

Published online: 16 August 2018

CTCs in a pulsatile manner, mimicking the periodic movement of the blood flow in human arteries. With this system, we found that high levels of SS, such as the levels present in arteries (15–30 dyne/cm^2), could elevate the levels of reactive oxygen species (ROS) in CTCs, which damaged their mitochondria and induced them to undergo apoptosis. In contrast, low levels of SS, such as the levels present in veins (5 dyne/cm^2), devoid of such an effect [13]. These findings raised a question of whether the ROS generated in CTCs in the circulation affect their sensitivity to anti-cancer drugs.

To address this question, we chose four anti-cancer drugs: doxorubicin (DOX), cisplatin, Taxol, and etoposide. These drugs were applied to cancer cells either under static conditions or in a circulatory environment. Their efficacy in inducing apoptosis and reducing cell viability was determined in three types of cancer cells, including breast, lung, and cervical cancer. The results show that the ROS-generating drugs DOX and cisplatin produced significantly stronger anti-cancer effects in CTCs from all three types of cancer, while the non-ROS-generating drugs, Taxol and etoposide, did not have such an effect. These findings suggest that ROS-generating drugs may be more effective in destroying CTCs in the vascular system. Upon validation in clinical studies, the results of this study may cause a paradigm shift in the use and dosing of these anti-cancer drugs to destroy CTCs during cancer therapy.

Materials and methods

Cell lines and cell culture

The MDA-MB-231 breast cancer cell line was provided by Professor Xiaofeng Le while he was working in the Department of Experimental Therapeutics at the M.D. Anderson Cancer Center of the University of Texas, USA. MCF7 breast cancer cells, A549 lung cancer cells and HeLa cervical cancer cells were purchased from the American Type Culture Collection (ATCC, Manassas, VA, USA). Three cell lines expressing caspase sensors (MCF7-C3, 231-C3, and HeLa-C3 cells) were generated by transfecting a recombinant DNA that encodes the fusion protein CFP-DEVD-YFP [14] into MCF7 [15], MDA-MB-231 [15] and HeLa cells [14], respectively. As these sensor cells can emit more green light due to the effect of fluorescence resonance energy transfer (FRET) in live sensor cells and produce more blue light upon caspase-3 activation in apoptotic sensor cells, they can be used to reveal apoptosis in real time and in individual cells by changing their color from green to blue [13–15]. MDA-MB-231, A549, 231-C3, HeLa-C3, and MCF7-C3 cells were cultured in Dulbecco's modified Eagle's medium (DMEM, Thermo Fisher Scientific, Waltham, MA, USA). The culture media were supplemented with 10% fetal bovine serum (FBS, HyClone, Buckinghamshire, UK) and 1% penicillin/streptomycin (Thermo Fisher Scientific, Waltham, MA, USA). All cells were cultured with 5% CO_2 in a 37 °C incubator.

Microfluidic circulatory system

The design and construction of the microfluidic circulatory system have been described in our previous publications [13, 16, 17]. The core component of this system is the peristaltic pump (Ismatec, Wertheim, Germany), which can generate physiologically relevant pulsatile SS in micro tubing with a radius of 0.25 mm and a length of 1.5 m [13, 16, 17]. When CTCs are circulated in this system, they will encounter SS, which can be calculated using Poiseuille's equation: $\tau = \frac{4Q\eta}{\pi R^3}$, where Q is the flow rate in mL/sec, η is the dynamic viscosity of the culture medium, which equals 0.012 dynes sec/cm^2, and R is the inner radius of the tube (0.25 mm). An SS level of 15 dyne/cm^2 was used in this study, and that value is abbreviated as SS15.

Anti-cancer drugs

The anti-cancer drugs DOX, cisplatin, etoposide, and Taxol were purchased from Selleck Chemicals (Houston, TX, USA). The working concentrations of all four drugs were freshly prepared from their own stock solutions. The drugs were uniformly mixed with the cells in DMEM containing 10% FBS and 1% penicillin and streptomycin, pH 7.4 (PS, Gibco, USA), before being applied to the microfluidic circulatory system or added to each well of a 96-well culture plate. The cells that were treated with drugs were maintained at 37 °C in a 5% CO_2 incubator and were then collected at the designated time points for various analyses. All drug testing experiments were conducted in triplicate.

Antioxidants

The antioxidants N-acetylcysteine (NAC) and propyl gallate (PG) were purchased from Sigma, USA. The working concentrations of both antioxidants were freshly prepared from their stock solutions. The antioxidants NAC or PG and the ROS-generating anti-cancer drugs DOX or cisplatin were uniformly mixed with cells in DMEM containing 10% FBS and 1% penicillin and streptomycin, pH 7.4 (PS, Gibco, USA), before being applied to the microfluidic circulatory system. The cells that were treated with drugs and antioxidants were maintained at 37 °C in a 5% CO_2 incubator and were then collected at the designated time points for various analyses. All experiments testing the combined effects of antioxidants and drugs were conducted in triplicate.

Using FRET microscopy to detect apoptosis in a microfluidic circulatory system

The rate of apoptosis was determined using fluorescence resonance energy transfer (FRET) microscopy. An inverted Zeiss Axiovert S100 fluorescence microscope (Carl Zeiss, Germany) and a computer-controlled charge-coupled device (CCD) camera (AxioCam MRm, Carl Zeiss, Germany) were used to capture the FRET images [13, 14, 16]. The cells were excited with a wavelength of 436 ± 10 nm, and two emission wavelengths, one from cyan fluorescent protein (CFP) (480 ± 20 nm) and another from yellow fluorescent protein (YFP) (535 ± 15 nm), were individually captured. The Image-Pro Plus software (Media Cybernetics, Inc., USA) was used to merge the digital fluorescence images of CFP and YFP.

In the merged FRET images, live cells appeared in green color while apoptotic cells appeared in blue color. This difference occurs because in the live cells, the fusion protein CFP-DEVD-YFP is intact and emits more green fluorescence. In sensor cells undergoing apoptosis, caspase-3 is activated, resulting in the cleavage of the peptide linker at the DEVD sequence between CFP and YFP. As a result of the separation of CFP from YFP, the energy cannot be transferred from the CFP donor to the YFP acceptor. Consequently, the color of the merged FRET image changes from green to blue, indicating apoptosis [13, 14, 16]. The merged FRET images were analyzed to calculate the percentage of apoptotic cells using the following formula:

$$\%\ \text{of apoptotic cells} = \frac{\text{Total number of blue cells}}{\text{Total number of green and blue cells}}$$

Measurement of cell death by annexin V and propidium iodide (PI) staining

To detect apoptotic cell death in A549 lung cancer cells that do not express our caspase sensor C3, annexin V and PI staining were used. Phosphatidylserine (PS) is located in the inner layer of a cell membrane in normal cells. However, in apoptotic cells, PS translocates from the inner to outer layer of the cell membrane, and this change can be used to indicate apoptosis. Annexin V is a 35–36 kDa calcium-dependent phospholipid-binding protein that can bind PS exposed to the outer layer of the cell membrane. After various circulatory and drug treatments, the cells were collected by centrifugation at 1500 rpm for 3 min, washed twice with cold PBS and resuspended in 1X annexin-binding buffer. For every 100 µL of cell suspension, 10 µL of annexin V solution (Thermo Fisher Scientific, Waltham, MA, USA) and 2 µL of PI at 100 µg/mL (Sigma, USA) were added and incubated for 30 min at room temperature in the dark. The cells were washed with 1× annexin-binding buffer. Annexin V and PI fluorescence was immediately observed under an inverted fluorescence microscope (Axio Observer Z1, Carl Zeiss, Germany). The cells that had an annexin V+/PI− staining pattern were considered to be in early apoptosis, while cells with an annexin V+/PI+ pattern were considered to be in late apoptosis or necrosis.

Calculation of cell viability using the MTT assay

After treatment with circulation under SS15 and drugs, the cells were collected from the circulatory system at the designated time points. Then, 100 µL of suspended cells was added to each well of a 96-well culture plate, followed by the addition of a sterilized MTT solution (5 mg/mL) [3-(4,5-dimethylthiazol-2-yl)-2,5-diphenyltetrazolium bromide] (Sigma-Aldrich, USA). After 3 h of incubation, 100 µL of a solubilization solution containing 10% sodium dodecyl sulphate (SDS) and 0.01 M HCl was added to each well to solubilize the formed formazan. After an overnight incubation, the optical density at 595 nm was measured using a plate reader (Perkin-Elmer Victor^3, USA).

Detection of intracellular ROS levels using 2′,7′-dichlorofluorescin diacetate (DCFDA)

MDA-MB-231 cells were treated with or without different drugs and circulated or left under static conditions in Fluoro-brite medium (Thermo Fisher Scientific, Waltham, MA, USA) containing 10% FBS (HyClone, Buckinghamshire, UK) for 3 h. Then, the cells were collected and centrifuged to remove various drugs. The cells were immediately stained with 10 µM CM-H2DCFDA (DCFDA) (Thermo Fisher Scientific, Waltham, MA, USA) prepared in Fluoro-brite medium. After incubation for 30 min, the medium with DCFDA was removed, and the cells were resuspended in fresh Fluoro-brite medium. Then, 100 µL of Fluoro-brite medium containing cells was added to 96-well plates. Green fluorescence images of DCFDA were immediately captured using an inverted fluorescence microscope (Axio Observer Z1, Carl Zeiss, Germany) at an excitation wavelength of 495 nm and an emission wavelength of 529 nm. Five images were collected for each condition, and the average value of fluorescence intensity was calculated from these images using ZEN software.

Analysis of the superoxide formation by dihydroethidium (DHE) staining

MDA-MB-231 cells were treated with or without different drugs, circulated or left under a static condition in Fluoro-brite medium (Thermo Fisher Scientific, Waltham, MA, USA) containing 10% FBS (Hyclone, Buckinghamshire, UK) for 3 h; after which the cells were collected and centrifuged to remove various drugs. The cells were immediately

stained with 10 μM dihydroethidium (DHE) (Thermo Fisher Scientific, Waltham, MA, USA) prepared in Fluoro-brite medium. After incubation for 30 min, the medium with DHE was removed and cells were re-suspended in fresh Fluoro-brite medium. Then, 100 μL of Fluoro-brite medium containing cells were added in 96-well plates. The red fluorescent images of DHE were captured using an inverted fluorescence microscope (Axio Observer Z1, Carl Zeiss, Germany) at an excitation wavelength of 535 nm and an emission wavelength of 610 nm. Five images were taken for each condition and the average value of fluorescence intensity was calculated from these images using ZEN software.

Statistical analysis

All sets of data are presented as the means ± standard deviations from at least three independent sets of experiments. We analyzed statistical significance using Student's *t* test for two-tailed distributions with two-sample unequal variance to calculate the *p* values between two groups. We considered *p* values of $*p < 0.05$, $**p < 0.01$, and $***p < 0.001$ to be statistically significant. To determine the rate of apoptosis, we calculated the rate using FRET images of at least 300 cells obtained from three independent experiments.

Results

Physiological fluidic SS significantly enhanced the anti-cancer efficacy of DOX in estrogen receptor (ER)+ breast cancer cells

DOX is widely used as the first-line chemotherapeutic agent to treat numerous types of cancers, including breast, ovarian, bladder, lung, thyroid, and stomach cancers, neuroblastoma, Wilms' tumor, lymphoma, some acute leukaemia, and Kaposi's sarcoma [18–21]. It is well documented that DOX uses two mechanisms to achieve its anti-cancer effect. The first mechanism is to damage DNA by inhibiting topoisomerase, which arrests the cells in S phase and further induces apoptosis [22, 23]. The second mechanism is to produce superoxide, which can damage mitochondria and induce apoptosis [13, 24]. In our previous study, we showed that pulsatile SS elevated the levels of ROS, including superoxide and hydrogen peroxide, in circulated breast cancer cells [13, 17]. We thus hypothesized that these SS-elevated ROS can further increase the apoptotic effect of DOX.

To test this hypothesis, we compared the cytotoxic effects of DOX on ER+ MCF7 breast cancer cells under static or circulatory conditions. To detect apoptotic cell death immediately after the circulatory process, we used engineered MCF7-C3 sensor cells that can detect apoptosis in real time [13, 15]. The sensor cells were circulated in our microfluidic circulatory system under a pulsatile SS of 15 dyne/cm^2 for 12 h. We used SS15, as this value represents the average level of SS in a human artery in the resting state [25, 26]. Four experimental conditions were designed for this study: (1) circulation under SS15 for 12 h; (2) No SS, but treatment with 2.5 μM DOX for 12 h on an adhesive surface; (3) No SS, but treatment with 2.5 μM DOX for 12 h on a non-adhesive surface, which was generated by pre-coating a 96-well plate with 1% Pluronic F-127 for 30 min, to reveal the potential damaging effects of detachment that can occur during circulation; and (4) Circulating cells under SS15 with 2.5 μM DOX for 12 h.

After various treatments, the MCF7-C3 cells were collected and subjected to phase microscopy and FRET imaging analysis. The fluorescence micrographs in Fig. 1a show that DOX significantly reduced the number of green live cells and increased the number of blue apoptotic cells when it was applied to MCF7-C3 cells under circulatory conditions at SS15 for 12 h. The quantified FRET images revealed that co-treatment with SS15 + 2.5 μM DOX for 12 h resulted in 78.2% apoptotic cell death, while single treatment produced much lower apoptotic rates ranging from 14.2% for SS15-12 h and 16.2% for 2.5 μM DOX on an adhesive surface to 20.3% for 2.5 μM DOX on a non-adhesive surface (Fig. 1b).

To confirm the above results, we used an MTT assay to measure the viability of MCF7-C3 cells under the same conditions. The graph in Fig. 1c shows that single treatment resulted in high cell viabilities under all three conditions: 64.0% for SS15-12 h; 73.6% for 2.5 μM DOX-12 h on an adhesive surface; and 60.0% for 2.5 μM DOX-12 h on a non-adhesive surface. However, co-treatment with SS15 + 2.5 μM DOX for 12 h reduced the cell viability to 17.3%. These results confirm that fluidic SS can significantly improve the cytotoxic effect of DOX on ER+ breast cancer cells during circulation.

Fluidic SS increased the anti-cancer efficacy of DOX against metastatic triple-negative breast cancer cells

To determine whether fluidic SS can also enhance the anti-cancer effect of DOX in metastatic breast cancer cells, we used engineered MDA-MB-231-C3 (231-C3) sensor cells [15]. MDA-MB-231 is a commonly used metastatic breast cancer cell line that does not express therapeutic receptors, including ER, progesterone receptor (PR), and human epidermal growth factor receptor 2 (HER2). As such, triple-negative breast cancer is not sensitive to hormone or HER2 therapy and is routinely treated with traditional chemotherapeutic agents, such as DOX and Taxol. More importantly, triple-negative breast cancer has the highest rate of metastasis and the lowest rate of survival compared to ER+ and HER2+ breast cancer. Furthermore, we confirmed that these

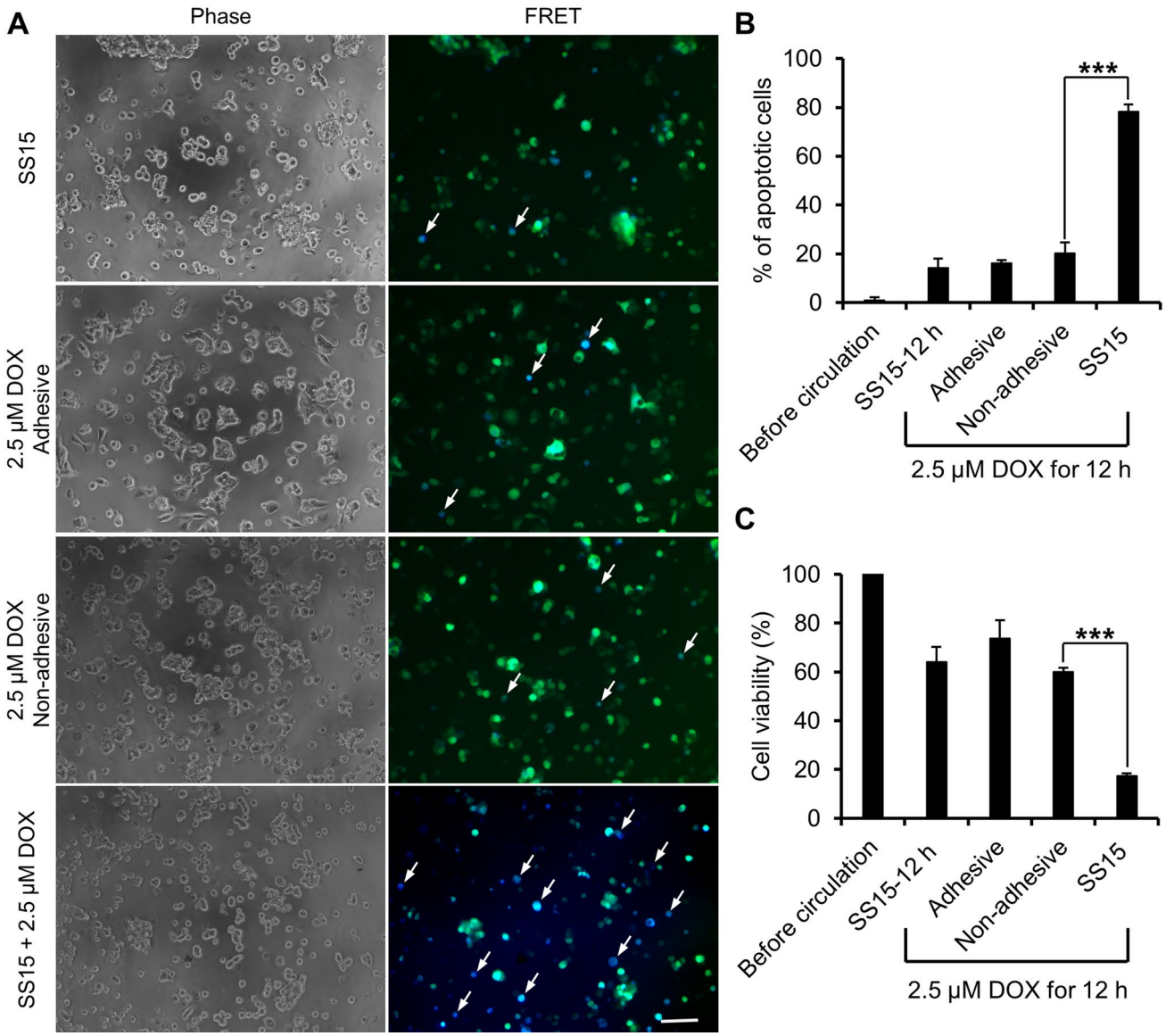

Fig. 1 Shear force improved the anti-cancer efficacy of DOX in ER+ MCF7-C3 breast cancer cells. **a** Optical micrographs of phase and FRET images showing the effects of single or co-treatment with SS15 and 2.5 μM DOX on MCF7-C3 cells for 12 h. Scale bar: 100 μm. **b** The apoptotic rate was quantified based on FRET imaging analysis. $N \geq 300$ cells for each group. **c** Cell viability was determined by an MTT assay. The results were normalized to the condition before circulation. $^{***}p < 0.001$ by Student's t test

231-C3 sensor cells retained their metastatic ability, as they could form metastatic tumors in the lungs of nude mice after being administered via intravenous injection [13].

In this experiment, 231-C3 cells were treated with the same four experimental conditions used for MCF7-C3 cells and subjected to phase microscopy and FRET imaging analysis. The FRET images in Fig. 2a show that for the cells treated with SS15 or 2.5 μM DOX alone, most cells appeared in green color; while for the cells treated with 2.5 μM DOX for 12 h under circulatory conditions, many cells appeared in blue color. The quantified FRET images revealed a low apoptosis rate of 4.8% for the SS15-12 h group; rates of 10.0 and 8.3% were obtained for the 2.5 μM DOX-12 h groups under adhesive and non-adhesive conditions, respectively (Fig. 2b). In contrast, the apoptotic rate of the co-treatment group (SS15 + 2.5 μM DOX-12 h) was 66.7%, which was eightfold higher than the apoptotic rate of cells treated with 2.5 μM DOX alone (Fig. 2b).

We further validated these findings by measuring the viability of 231-C3 cells using an MTT assay. The quantified results showed that single treatment with 2.5 μM DOX for 12 h generated high viabilities of 73.3% under adhesive conditions and 70.3% under non-adhesive conditions. In contrast, co-treatment with SS15 + 2.5 μM DOX for 12 h

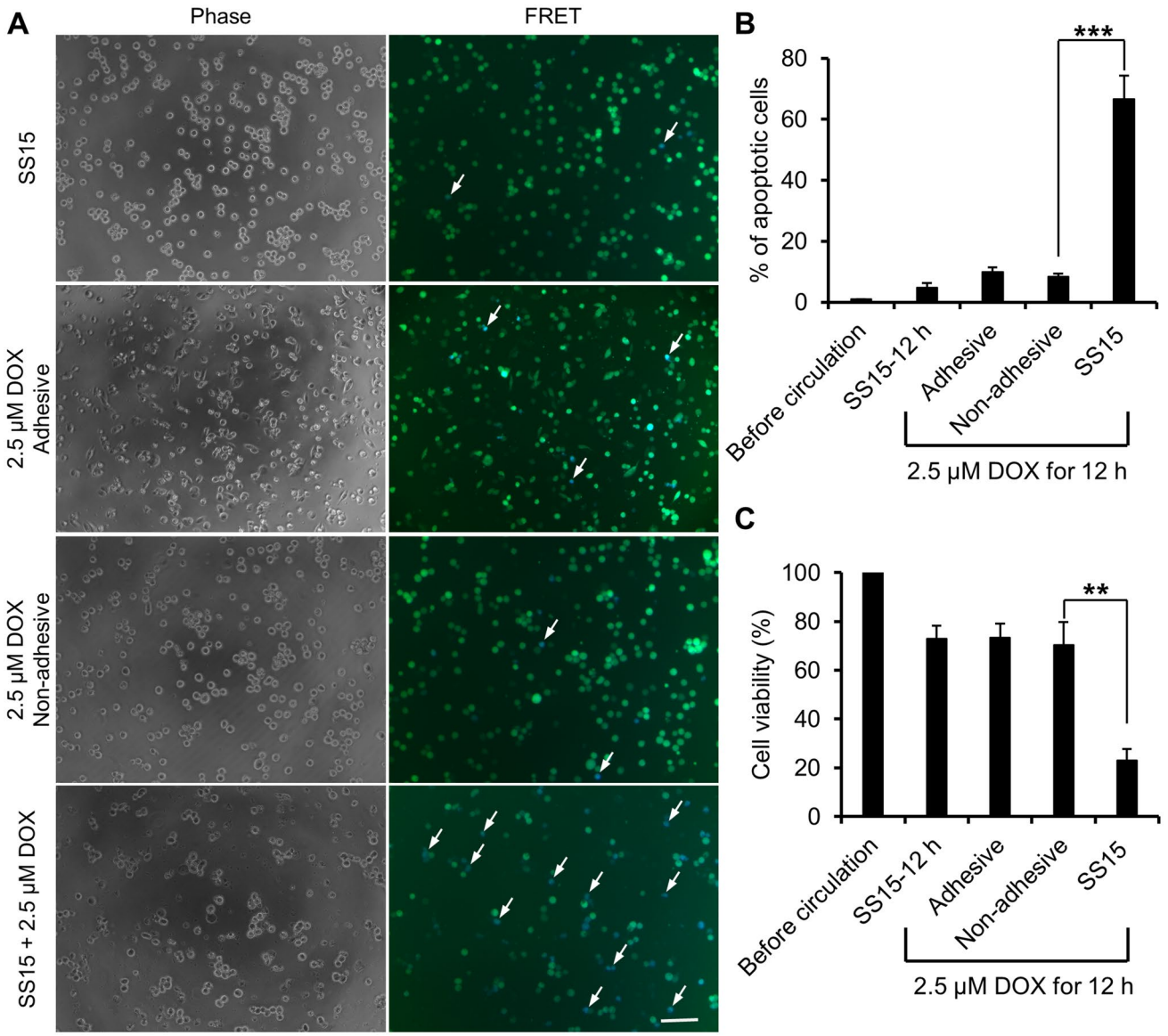

Fig. 2 Shear stress significantly enhanced the anti-cancer efficacy of DOX in metastatic 231-C3 cells. **a** Optical micrographs of phase and FRET images showing the effects of single or co-treatment with SS15 and 2.5 μM DOX on 231-C3 cells for 12 h. Scale bar: 100 μm. **b** The apoptotic rate was quantified based on FRET imaging analysis. $N \geq 300$ cells for each group. **c** Cell viability was determined by an MTT assay. The results were normalized to the condition before circulation. $^{**}p < 0.01$, $^{***}p < 0.001$ by Student's *t* test

produced a much lower cell viability of 23.0% (Fig. 2c). Taken together, these results indicate that physiological fluidic SS can increase the efficacy of DOX in metastatic breast cancer cells.

SS elevated the levels of ROS in DOX- and cisplatin-treated breast cancer cells

The observation that DOX exhibited a much stronger cytotoxic effect under circulatory conditions led us to hypothesize that co-treatment with DOX and circulation may produce more ROS in circulated cells. To test this hypothesis, we measured the level of hydrogen peroxide using the ROS indicator DCFDA. DCFDA is a fluorescent dye that emits a very low level of fluorescence inside cells; the presence of hydrogen peroxide can convert DCFDA into DCF, which emits much stronger green fluorescence. Thus, the intensity of green fluorescence can indicate the level of ROS [27]. Using this dye, we previously showed that circulating MDA-MB-231 cells under SS15 for 1–6 h significantly elevated the intracellular level of ROS [13, 17].

In this study, MDA-MB-231 cells were treated with or without 2.5 μM DOX under static or circulatory conditions

at SS15 for 3 h. The cells were collected after various treatments and immediately stained with 10 μM CM-H2DCFDA (DCFDA) prepared in Fluoro-brite medium for 30 min. The green fluorescence of DCF was captured using an inverted fluorescence microscope at an excitation wavelength of 495 nm and an emission wavelength of 529 nm. The fluorescence micrographs showed that more cells emitted green fluorescence after they were treated with either 2.5 μM DOX or circulated under SS15 for 3 h than after they were left untreated, demonstrating that both conditions increased ROS (Fig. 3a). Significantly, many more cells emitted green fluorescence when they were treated with 2.5 μM DOX under circulatory conditions (Fig. 3a). The fluorescence intensities were measured using the ZEN software. The quantified results showed that single treatment with SS15 or 2.5 μM DOX increased the level of ROS by 5.27- or 4.55-fold, respectively, while co-treatment with SS15 + DOX produced a much higher level of ROS elevation (15.16-fold increase) (Fig. 3b, d). These data may explain why DOX exhibited much stronger anti-cancer potency when it was applied to cancer cells under circulatory conditions.

To validate the synergistic effect of SS and ROS-generating drugs on ROS production, we compared the levels of ROS in MDA-MB-231 cells treated with three additional anti-cancer drugs (cisplatin, Taxol and etoposide) under static or circulatory conditions at SS15 for 3 h. The fluorescence images show that under static conditions, cisplatin increased the number of green fluorescent cells, while Taxol and etoposide did not; this finding indicates that cisplatin is a ROS-generating agent, while the other two anti-cancer drugs are non-ROS-generating agents (Fig. 3a). More importantly, among the three anti-cancer drugs tested, only co-treatment with cisplatin and SS15 for 3 h resulted in more cells that emitted green fluorescence corresponding to 13.56-fold increase in ROS level (Fig. 3a). In contrast, cells treated with Taxol or etoposide under circulatory conditions compared to the single treatment of SS15 for 3 h showed no increase in ROS level (Fig. 3c). These results suggest that fluidic SS and ROS-generating drugs, such as DOX and cisplatin, can synergistically increase the intracellular level of ROS in CTCs.

We also applied another commonly used ROS detecting dye, dihydroethidium (DHE) to measure ROS levels in circulated cancer cells. DHE can be oxidized by superoxide to produce 2-hydroxyethidium or ethidium. This oxidation process generates a bright red fluorescence. We treated the MDA-MB-231 cells with no drugs as a control and DOX, cisplatin, Taxol, and etoposide for 3 h. After which, the cells were stained with 10 μM DHE prepared in Fluoro-brite medium for 30 min and images were captured using an inverted fluorescence microscope at an excitation wavelength of 535 nm and an emission wavelength of 610 nm. The fluorescence micrographs indicate that DOX and cisplatin-treated cells produced more superoxide radicals indicating DOX and cisplatin are ROS generating agents, whereas etoposide and Taxol are not.

In order to validate the results based on DCFDA, we performed another experiment where cells were circulated under SS15 treated with 2.5 μM DOX, 100 μM cisplatin, 100 nM Taxol, and 100 μM etoposide for 3 h. After which, the cells were stained with 10 μM DHE for 30 min. The fluorescence micrographs showed that more cells emitted red fluorescence after they were treated with SS15 and 2.5 μM DOX for 3 h (Fig. 4a) than the individual treatment. The results were further quantified to determine the fold change in DHE. The single treatment with SS15 or 2.5 μM DOX increased the level of ROS by 3.85- or 4.56-fold, respectively, while co-treatment with SS15 + DOX produced a much higher level of ROS elevation (13.50-fold increase) (Fig. 4b, d). These data are consistent with the DCFDA results (Fig. 3b, d).

Then again, we compared the superoxide generation in MDA-MB-231 cells treated with SS15 together with three additional anti-cancer drugs (cisplatin, Taxol, and etoposide) for 3 h. Consistence with the DCFDA data above, co-treatment of cisplatin and SS15 for 3 h resulted in more cells that emitted red fluorescence corresponding to 9.50-fold increase in ROS level (Fig. 4a). In contrast, cells treated with Taxol or etoposide under circulatory conditions showed no increase in ROS level, compared to the single treatment of SS15 for 3 h (Fig. 4c, d). These results further confirm that SS treatment elevated the ROS levels in DOX- and cisplatin-treated breast cancer cells.

Cisplatin displayed stronger destructive effect against cancer cells in circulation

We then compared the killing effect of cisplatin in 231-C3 cells under static and circulatory conditions. For the static condition, 100 μM cisplatin was added to 231-C3 cells grown in either an adhesive or a non-adhesive 96-well plate and incubated for 12 h. For the circulatory condition, 100 μM cisplatin was added to 231-C3 cells, and the drug-cell suspension was circulated in our microfluidic system under SS15 for 12 h. The treated cells were then collected and processed for phase and FRET imaging analyses. The FRET images indicated that many cells were alive after being treated with 100 μM cisplatin for 12 h under static conditions. However, many blue apoptotic cells were observed after treatment with 100 μM cisplatin for 12 h under circulatory conditions with SS15 (Fig. 5a). We calculated the rate of apoptotic cells from the FRET images and found that treating cells with 100 μM cisplatin for 12 h resulted in 6.4 and 6.2% apoptosis for cells grown on adhesive or non-adhesive surfaces, respectively (Fig. 5b). However, the combined 12 h treatment with 100 μM cisplatin and SS15 enhanced the apoptotic rate by sevenfold to 44.6% in 231-C3 cells (Fig. 5b).

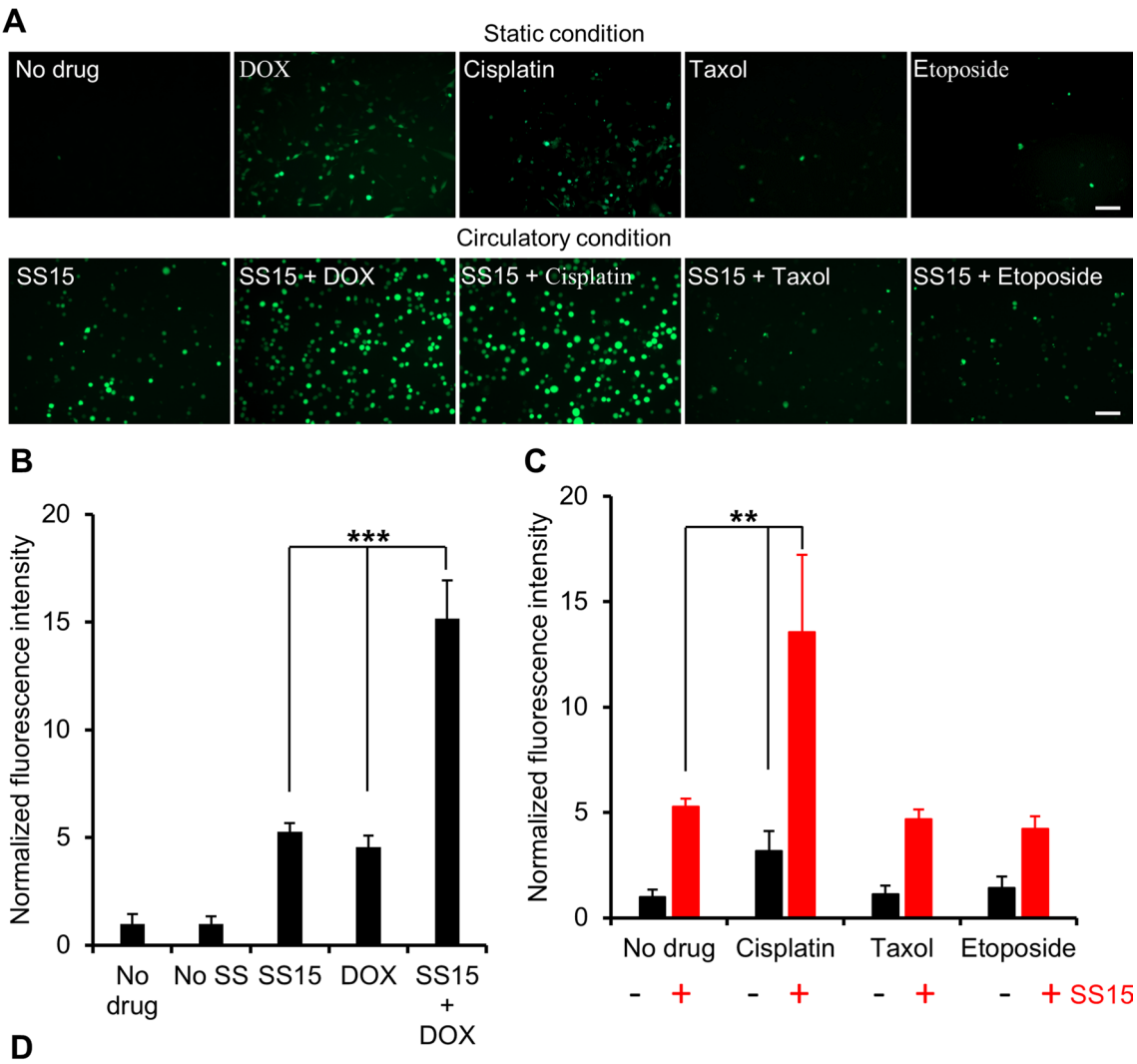

D

No	Condition	Fold change in DCFDA	
		Static condition	Circulatory condition
1	No drug - 3 h	1.00	5.27
2	2.5 μM DOX - 3 h	4.55	15.16
3	100 μM cisplatin - 3 h	3.18	13.56
4	100 nM Taxol - 3 h	1.12	4.68
5	100 μM etoposide - 3 h	1.42	4.22

Fig. 3 Shear stress only elevated the ROS levels in DOX- and cisplatin-treated cells. **a** Fluorescent images of MDA-MB-231 cells treated with various anti-cancer drugs under static or circulatory conditions at SS15 for 3 h. Scale bar: 100 μm. **b** and **c** Quantified fluorescence intensity of DCF from the cells in each group. $N \geq 300$ cells for each group. **d** The results were normalized to no drug treatment before circulation, and the fold changes in fluorescence intensity are presented in this panel. $^{**}p < 0.01$, $^{***}p < 0.001$ by Student's *t* test

To validate the findings obtained from FRET-imaging-based apoptotic analysis, MTT assay was performed. The graph in Fig. 5c shows that 231-C3 cells treated with 100 μM cisplatin for 12 h under static conditions retained high cell viability values of 86.5 and 94.0% on adhesive and non-adhesive surfaces, respectively (Fig. 5c).

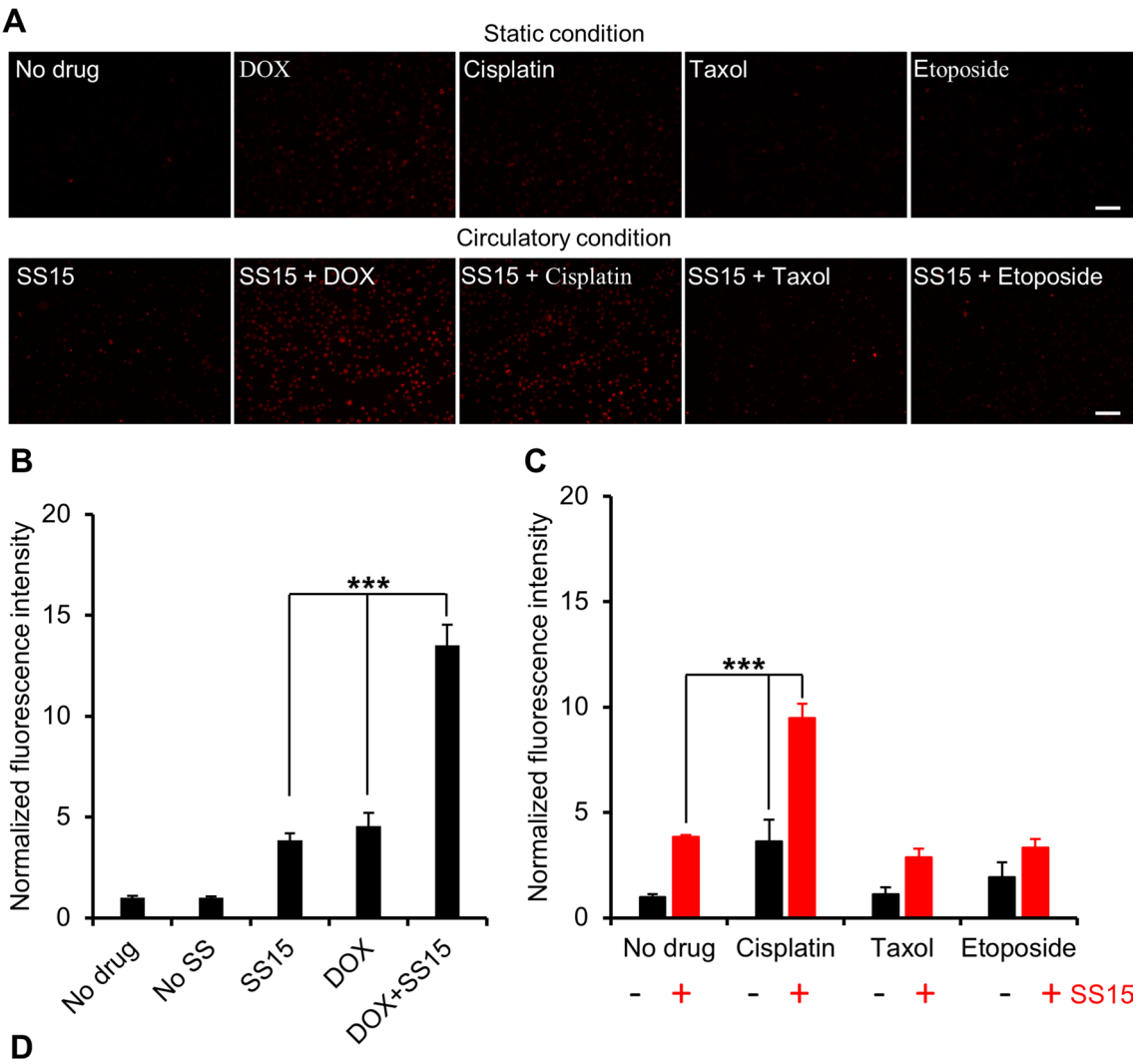

D

No	Condition	Fold change in DHE	
		Static condition	Circulatory condition
1	No drug - 3 h	1.00	3.85
2	2.5 μM DOX - 3 h	4.56	13.50
3	100 μM cisplatin - 3 h	3.63	9.50
4	100 nM Taxol - 3 h	1.12	2.88
5	100 μM etoposide - 3 h	1.94	3.34

Fig. 4 Shear stress increases the production of ROS in DOX- and cisplatin-treated cells. **a** Fluorescent images of MDA-MB-231 cells treated with various anti-cancer drugs under static or circulatory conditions at SS15 for 3 h stained with DHE. Scale bar: 100 μm. **b** and **c** Quantified fluorescence intensity of DHE from the cells in each group. $N \geq 300$ cells for each group. **d** The fold changes in fluorescence intensity are presented in this panel and the results were normalized to no drug treatment and before circulation, $^{***}p < 0.001$ by Student's *t* test

In contrast, co-treatment of 231-C3 cells with 100 μM cisplatin for 12 h under circulation at SS15 significantly reduced the cell viability to 45.8% (Fig. 5c). These results demonstrate that SS can also effectively increase the anti-cancer effect of another ROS-generating drug, cisplatin, in circulation.

Fluidic SS did not enhance the anti-cancer effect of Taxol and etoposide in circulation

In Figs. 3 and 4, we showed that neither Taxol nor etoposide increased ROS in MDA-MB-231 cells under circulatory conditions. We thus predicted that the efficacy of these two anti-cancer drugs against CTCs might not be affected by SS treatment. To test this prediction, we treated 231-C3 cells with either 100 nM Taxol or 100 μM etoposide for 12 h under static or circulatory conditions. We then used FRET-based imaging analysis to determine their apoptotic rates and MTT assay to measure their viabilities. The results presented in Fig. 6 demonstrate that neither Taxol nor etoposide caused significant cell damage either alone or when applied in circulation for 12 h. In particular, the

Fig. 6 Comparison of the anti-cancer effects of Taxol and etoposide under static and circulatory conditions. **a** Phase and merged FRET images of 231-C3 cells before circulation and after 12 h of treatment with 100 nM Taxol or 100 μM etoposide on a non-adhesive surface or in circulation under SS15. Scale bar: 100 μm. **b** The percentage of apoptotic cells was quantified from at least 300 cells for each condition. **c** The cell viability was measured using an MTT assay for the same conditions. The results were normalized to the condition before circulation ▶

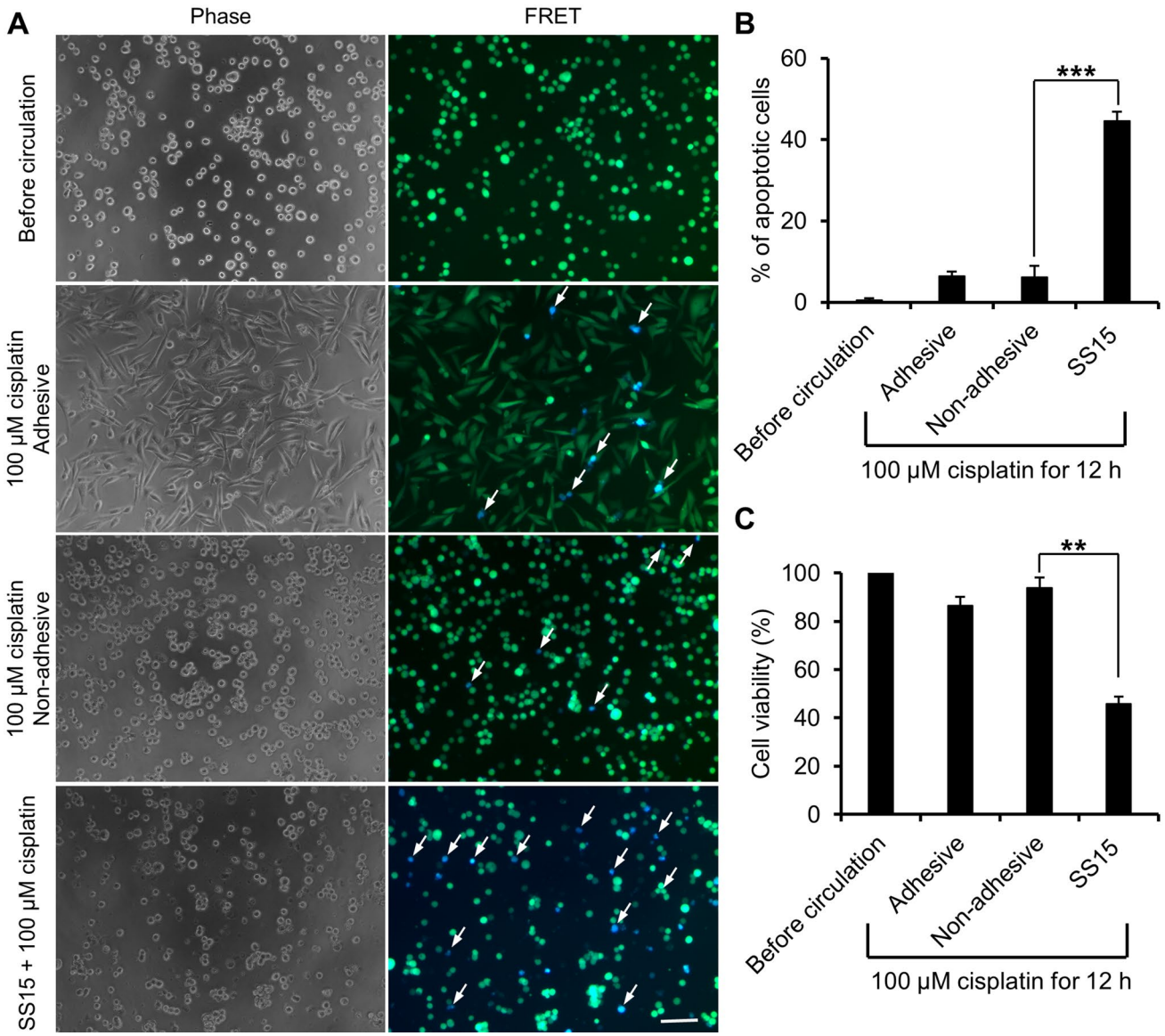

Fig. 5 Cisplatin displayed a much stronger killing effect against circulated 231-C3 cells. **a** Optical micrographs of phase and FRET images from 231-C3 cells treated with 100 μM cisplatin for 12 h under static conditions on an adhesive or non-adhesive surface or in circulation at SS15. Scale bar: 100 μm. **b** The apoptotic rate was quantified based on FRET imaging analysis. $N \geq 300$ cells for each group. **c** Cell viability was determined by an MTT assay. The results were normalized to the condition before circulation. $^{**}p < 0.01$, $^{***}p < 0.001$ by Student's *t* test

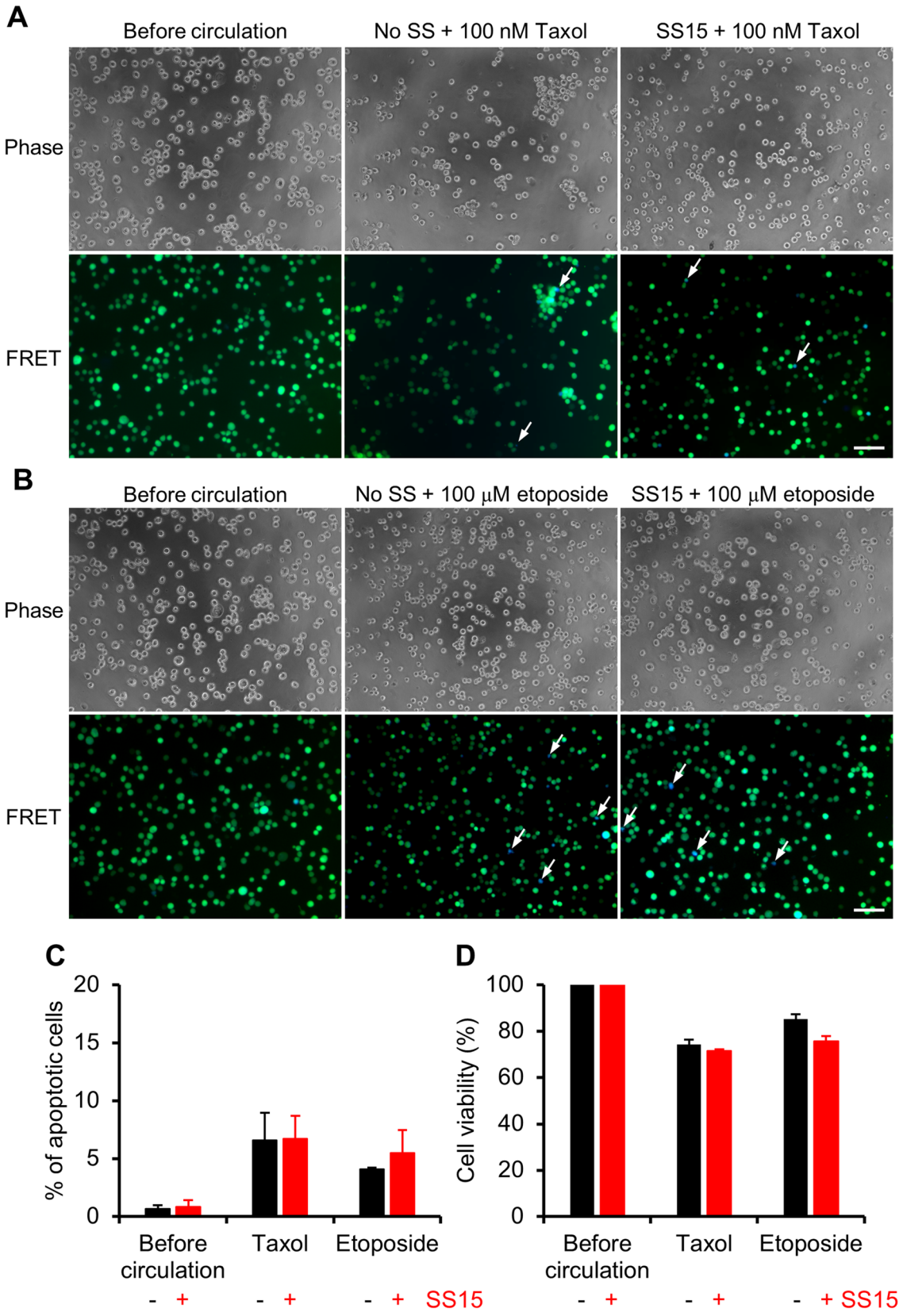

apoptotic rate obtained after 100 nM Taxol treatment under static conditions on a non-adhesive surface was 6.6%, and the apoptotic rate obtained with 100 nM Taxol in circulation at SS15 was 6.7% (Fig. 6a, c). Similarly, low apoptotic rates were obtained after single treatment with 100 μM etoposide for 12 h (4.1%) and after co-treatment with etoposide and SS15 (5.5%) (Fig. 6a, c).

We further validated the results of the apoptotic analysis with those obtained in a cell viability assay. High viabilities were detected in 231-C3 cells treated with 100 nM Taxol for 12 h under both static conditions on a non-adhesive surface (74.3%) and circulatory conditions at SS15 (71.5%) (Fig. 6d). Similarly, high viabilities were obtained from 231-C3 cells treated with 100 μM etoposide for 12 h under static conditions (85.3%) and in circulation (75.6%) (Fig. 6d). Taken together, these results showed that physiological levels of SS did not enhance the anti-cancer effect of non-ROS-generating drugs, such as Taxol and etoposide.

Antioxidants reduced the SS-stimulated anti-cancer effect of DOX and cisplatin

We have shown that the anti-cancer effects of DOX and cisplatin were significantly enhanced when they were applied to circulated cancer cells, and the elevation of ROS levels in CTCs was revealed as the mechanism of action. To validate the role of ROS in DOX- and cisplatin-mediated apoptosis in CTCs, we used two antioxidants, NAC, and PG, to suppress ROS generation. Metastatic 231-C3 breast cancer cells were treated with 2.5 μM DOX or 100 μM cisplatin in the presence of either 5 mM NAC or 20 μM PG and circulated under SS15 for 12 h. The cells were collected and examined by phase and FRET microscopy. The results in Fig. 7 show that co-treatment with SS15 and 2.5 μm DOX resulted in a high level of apoptosis (66.7%) in 231-C3 cells, which was significantly reduced to 12.1% and 12.9% by the addition of the 5 mM NAC and 20 μM PG, respectively. Similarly, co-treatment with SS15 and 100 μM cisplatin produced 44.6% apoptosis, which was significantly reduced to 7.5 and 5.7% after incubation with 5 mM NAC and 20 μM PG, respectively. These results show that repressing ROS elevation can attenuate the synergistic effect of SS15 and DOX or cisplatin, which indicates the crucial role of ROS elevation in DOX- and cisplatin-induced apoptosis in CTCs.

DOX and cisplatin also displayed stronger apoptotic effects in circulated lung and cervical cancer cells

To test the general application of the use of the ROS-generating drugs DOX and cisplatin to kill CTCs in circulation, we evaluated the destructive effects of these drugs on two more cancer cell lines: a lung cancer cell line (A549) and a cervical cancer cell line (HeLa-C3). A549 lung cancer cells were circulated in our microfluidic system under SS15 for 12 h with or without various anti-cancer drugs: 2.5 μM DOX, 100 μM cisplatin, 100 nM Taxol, and 100 μM etoposide. The cytotoxic effects of various treatments were determined by annexin V/PI staining, as described previously [28], since these A549 cells do not express the apoptotic sensor C3. Annexin V can bind to phosphatidyl serine and thus detect apoptotic cells, whereas PI can stain apoptotic or necrotic cells with damaged plasma membranes [29]. The results presented in Fig. 8a show that annexin V and PI were barely detectable in A549 cells before circulation, while weak signals from annexin V and PI were visible after SS15 treatment for 12 h. Very high green and red fluorescence intensities appeared in the cells after being circulated under SS15 for 12 h with either 2.5 μM DOX or 100 μM cisplatin, while minimal levels of fluorescence were observed in A549 cells treated with 100 nM Taxol or 100 μM etoposide in circulation for 12 h.

To further investigate the effects of DOX and cisplatin on apoptosis induction in CTCs under circulatory conditions, we utilized human cervical cancer cells (HeLa) expressing our apoptotic sensor (HeLa-C3) [14]. HeLa-C3 cells were circulated in our microfluidic system under SS15 for 12 h with or without 2.5 μM DOX or 100 μM cisplatin and analyzed by phase and FRET microscopy. The results presented in panels B and C show that the apoptotic rate obtained after treatment with 2.5 μM DOX was quite low at 19.8% under static conditions and was significantly increased to 80.4% under the circulatory condition of SS15 for 12 h (Fig. 8c). This value is close to the high apoptotic rate of 78.2% produced by co-treatment with SS15 + DOX in MCF7-C3 breast cancer cells (Fig. 1b). The circulatory condition also significantly increased the apoptotic rate of 100 μM cisplatin from 6.5% under static conditions to 55.0% in a circulatory environment in HeLa-C3 cells (Fig. 8c). These results confirm that DOX and cisplatin can also be used to effectively destroy CTCs derived from lung and cervical cancer.

Discussion

This study shows, for the first time, that ROS-generating drugs, such as DOX and cisplatin, exhibit much higher cytotoxicity in cancer cells circulated under fluidic conditions than do non-ROS-generating drugs, such as Taxol and etoposide. This discovery was made based on two important developments. The first is the development of a microfluidic circulatory system that can generate a pulsatile fluidic SS of 15 dyne/cm^2, which is the average SS in human arteries [13, 16]. The second is the finding that in

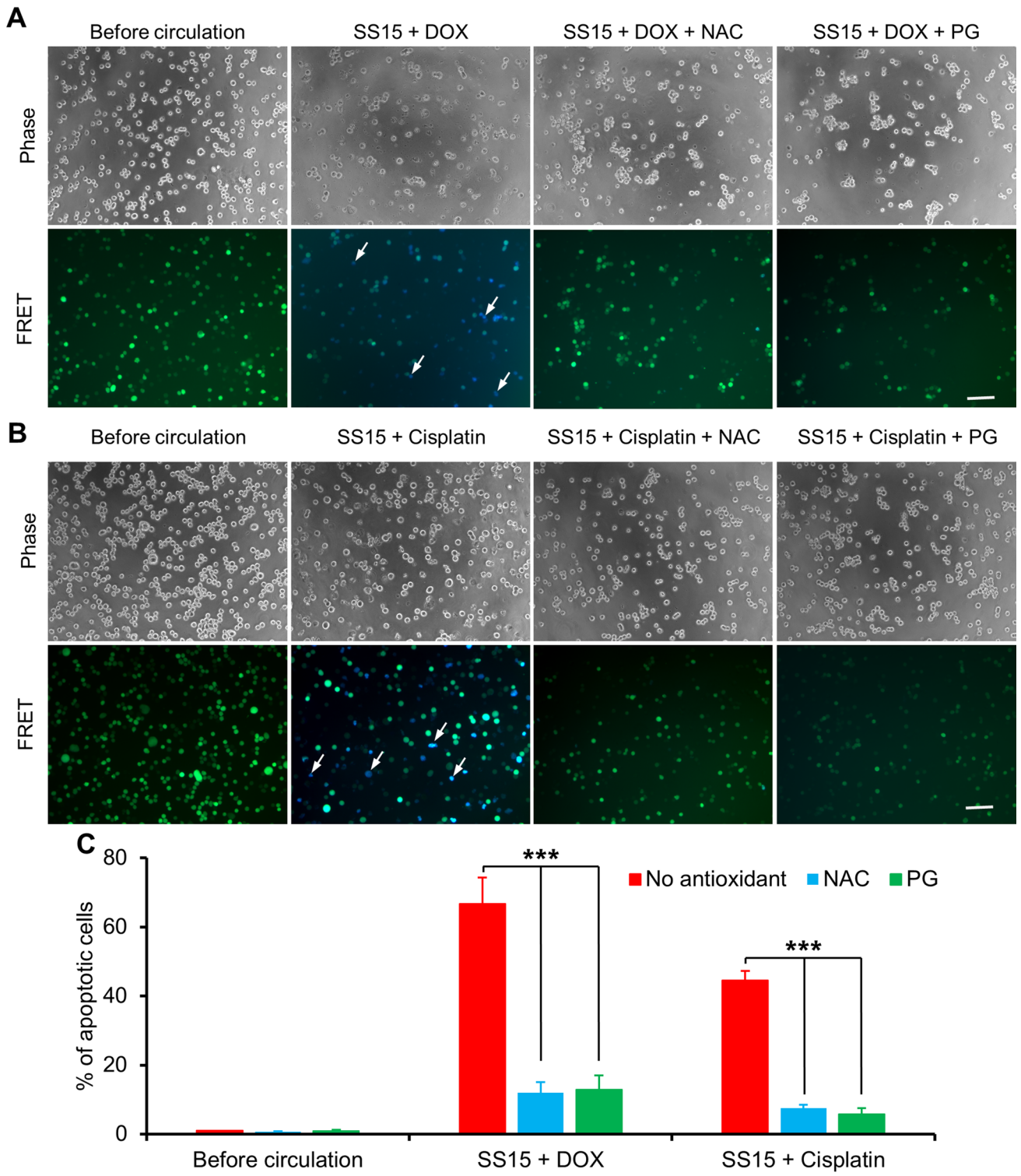

Fig. 7 Antioxidants significantly reduced the apoptotic effect of SS with DOX or cisplatin in 231-C3 cells. **a** and **b** Phase and FRET images of 231-C3 breast cancer cells after treatment with the following reagents alone or in combination: 2.5 μM DOX or 100 μM cisplatin with 5 mM NAC or 20 μM PG under circulatory treatment conditions conducted under SS15 for 12 h. Scale bar: 100 μm. **c** The percentage of apoptotic cells was quantified from FRET images of more than 300 cells for each group, ***$p < 0.001$ by Student's *t* test

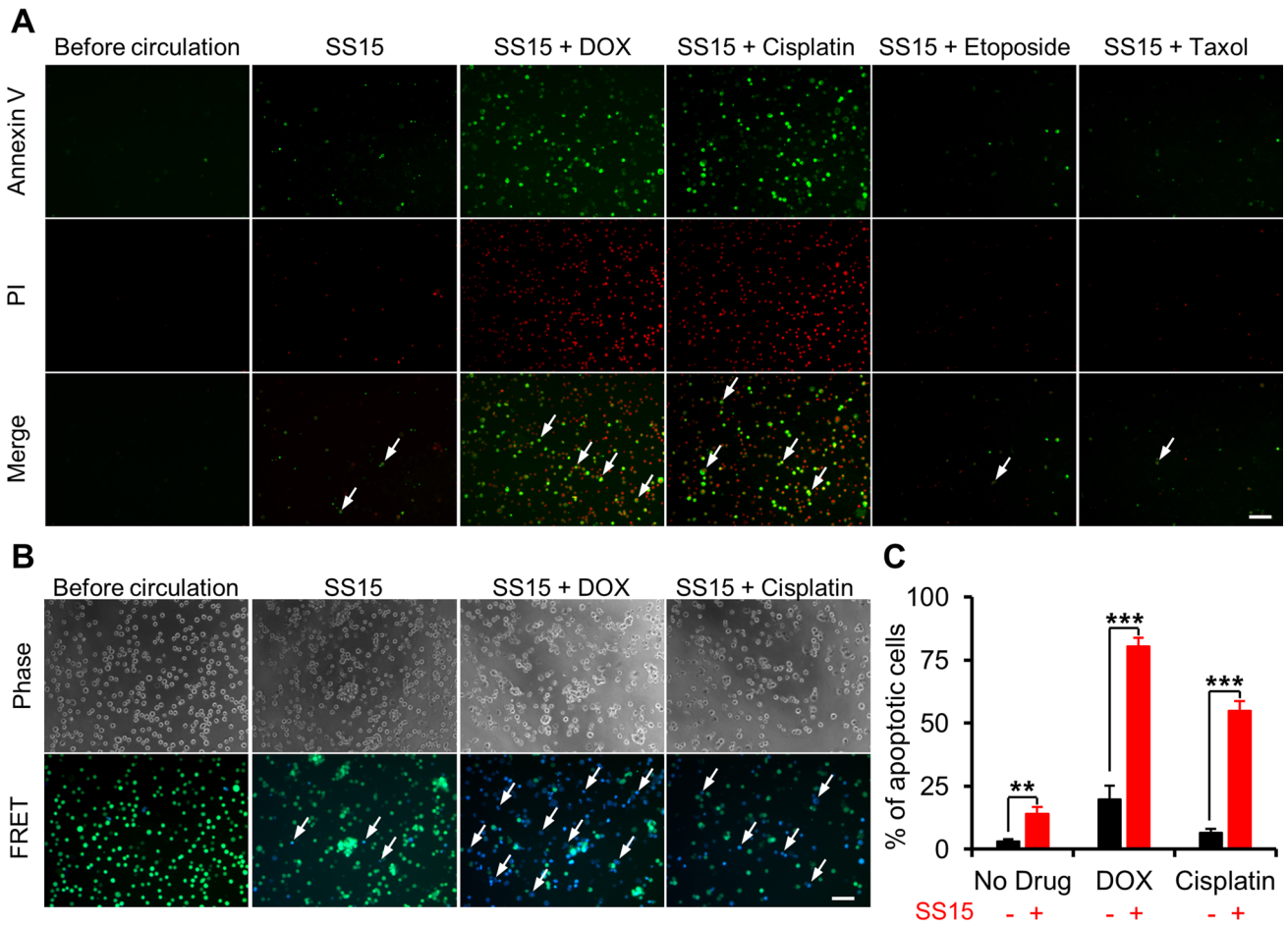

Fig. 8 Examining the effects of SS on drug efficacy in other types of cancer cell lines. **a** Annexin V and PI staining for detecting apoptosis in A549 cells. Overview of apoptotic status in the specified conditions: before circulation or after circulation under SS15 for 12 h with four anti-cancer drugs (2.5 μM DOX, 100 μM cisplatin, 100 μM etoposide or 100 nM Taxol). Scale bar: 100 μm. **b** Phase and FRET images of HeLa-C3 cells before circulation or after circulation under SS15 for 12 h with 2.5 μM DOX or 100 μM cisplatin. Scale bar: 100 μm. **c** The apoptotic rate of HeLa-C3 cells was quantified from FRET images under the same treatment conditions described in panel B. N ≥ 300 cells for each group, $^{**}p<0.01$, $^{***}p<0.001$ by Student's *t* test

this circulatory system, pulsatile SS elevated the levels of ROS in CTCs [13, 17]. By combining this new information and technology, we were able to address the following important question: can SS affect the efficacy of anti-cancer drugs in CTCs? The results showed that DOX and cisplatin displayed much stronger potency than Taxol and etoposide under circulatory conditions, but such differences were not observed under static treatment conditions.

Based on these findings, we suggest that cancer patients may benefit more from ROS-generating drugs, such as DOX and cisplatin, than non-ROS-generating drugs, such as Taxol and etoposide. The ROS-generating drugs can produce much higher levels of ROS in the circulation, which allows them to kill more CTCs in the vascular system. On the other hand, cancer patients should be careful when they consume antioxidants, as they may counteract the anti-cancer effects of ROS-generating drugs.

This new information may also help oncologists to design treatment strategies. For example, although both Taxol and DOX are first-line chemotherapeutic agents for treating breast cancer, there is no clear guideline concerning which drug should be used first in chemotherapy. If DOX is proven in clinical studies to produce much stronger anti-cancer efficacy in CTCs, DOX should be given to breast cancer patients before surgery, during which a large number of cancer cells may detach from the primary tumor and enter the vascular system to become CTCs.

In addition to the two ROS-generating drugs tested in this study, there are 20 more therapeutic agents available in the clinic or under clinical trials plus radiotherapy that can directly or indirectly generate ROS (Table 1). As some of these agents may also produce higher efficacy under fluidic SS conditions, their therapeutic effects on CTCs should be carefully examined.

Table 1 Information about therapeutics that can directly or indirectly generate ROS

Mechanism	Name	Targeted cancer types	Stage
Directly generate ROS	5-Fluorouracil	Colorectal cancer, head, and neck cancer	FDA-approved
	Cisplatin	Multiple types of cancer	
	Daunorubicin		
	Doxorubicin		
	Ionizing radiation		
Mitochondrial dysfunction	2-Methoxyestradiol	Prostate cancer and leukemia	
	Arsenic trioxide	Leukemia and myeloma	
	Lanperasone	$KRAS^{G12D}$-expressing tumor cells	
	N-(4-hydroxy-phenyl) retinamide	Prostate cancer, breast cancer, and neuroblastoma	
	N-benzyloxy-carbonyl-Ile-Glu (O-t-butyl)-Ala-leucinal	Leukemia	
	Erastin	RAS^{V12}-expressing tumor cells	Phase I/II
Perturb the ER stress pathway	Bortezomib	Multiple myeloma	FDA-approved
	Celecoxib	Colorectal and prostate cancer	
	Nelfinavir	Cervical and pancreatic cancer	
	G202	Liver and prostate cancer	Phase II
Alter GSSG/GSH levels	6-aminonicotinamide	Colon cancer	Phase I
	Buthionine sulphoximine	Ovarian and breast cancer, melanoma	Phase I
	Dibenzophenanthridine	Lymphoma and breast cancer	Preclinical
	L-aspariginase	Leukemia and pancreatic cancer	Phase II
	NOV-002	Lung, breast, and ovarian cancer	Phase III
	Sulphasalazine	Pancreatic and lung cancer	Phase I/II
Alter NADP/NADPH levels	AG-22	Advanced hematological malignancies	Phase II
	AGX-891	Glioma and leukemia	Preclinical

Furthermore, our microfluidic circulatory system can be used to study how CTCs behave under the combined effects of fluidic SS and anti-cancer drugs. These studies will provide new insights for developing novel strategies to specifically enhance the destruction of CTCs, thus effectively preventing metastasis.

Conclusion

Our results showed that DOX and cisplatin are more destructive to circulating tumor cells than are Taxol and etoposide. Further, the data revealed that DOX and cisplatin produced more reactive oxygen species (ROS) in CTCs whereas Taxol and etoposide did not elevate the levels of ROS in CTCs. Antioxidants abolished the apoptotic effects of DOX and cisplatin in CTCs. Our findings indicate, for the first time, that ROS-generating drugs are more potent for destroying CTCs than are non-ROS-generating drugs.

Acknowledgements This work was supported by the Ministry of Education, Singapore (Tier 2 Grant No.: MOE2014-T2-1-025) and The Science and Technology Development Fund of Macau (FDCT: 083/2016/A2). We would like to thank Prof. Xiao-feng Le for providing the MDA-MB-231 breast cancer cell line while he was working in the Department of Experimental Therapeutics at the University of Texas M.D. Anderson Cancer Center, Houston, TX, USA. We also want to thank the Singapore International Graduate Award (SINGA) for providing a PhD scholarship to Sagar Regmi.

Author contributions SR and KQL conceived and designed the experiments. SR performed the experiments. SR and KQL analyzed the data. SR, TSS, SL, and KQL contributed reagents/materials/analytical tools/project management. SR and KQL wrote the paper.

Compliance with ethical standards

Conflict of interest The authors have no conflict of interest to declare.

References

1. Wittekind C, Neid M (2005) Cancer invasion and metastasis. Oncology 69(Suppl. 1):14–16
2. Nicholson C, Vela I, Williams E (2017) Prostate cancer metastasis. Introd Cancer Metastasis 1:33–59
3. Longley D, Johnston P (2005) Molecular mechanisms of drug resistance. J Pathol 205(2):275–292
4. Chambers AF, Groom AC, MacDonald IC (2002) Dissemination and growth of cancer cells in metastatic sites. Nat Rev Cancer 2(8):563–572

5. Bernards R, Weinberg RA (2002) Metastasis genes: a progression puzzle. Nature 418(6900):823
6. Alix-Panabières C, Riethdorf S, Pantel K (2008) Circulating tumor cells and bone marrow micrometastasis. Clin Cancer Res 14(16):5013–5021
7. Hughes AD, King MR (2012) Nanobiotechnology for the capture and manipulation of circulating tumor cells. Wiley Interdiscip Rev 4(3):291–309
8. Allard WJ, Matera J, Miller MC, Repollet M, Connelly MC, Rao C, Tibbe AG, Uhr JW, Terstappen LW (2004) Tumor cells circulate in the peripheral blood of all major carcinomas but not in healthy subjects or patients with nonmalignant diseases. Clin Cancer Res 10(20):6897–6904
9. Cohen SJ, Punt CJ, Iannotti N, Saidman BH, Sabbath KD, Gabrail NY, Picus J, Morse MA, Mitchell E, Miller MC et al (2009) Prognostic significance of circulating tumor cells in patients with metastatic colorectal cancer. Ann Oncol 20(7):1223–1229
10. De Giorgi U, Mego M, Rohren EM, Liu P, Handy BC, Reuben JM, Macapinlac HA, Hortobagyi GN, Cristofanilli M, Ueno NT (2010) 18F-FDG PET/CT findings and circulating tumor cell counts in the monitoring of systemic therapies for bone metastases from breast cancer. J Nucl Med 51(8):1213–1218
11. Maheswaran S, Haber DA (2010) Circulating tumor cells: a window into cancer biology and metastasis. Curr Opin Genet Dev 20(1):96–99
12. Davnall F, Yip CS, Ljungqvist G, Selmi M, Ng F, Sanghera B, Ganeshan B, Miles KA, Cook GJ, Goh V (2012) Assessment of tumor heterogeneity: an emerging imaging tool for clinical practice? Insights Imaging 3(6):573–589
13. Fu A, Ma S, Wei N, Tan BXX, Tan EY, Luo KQ (2016) High expression of MnSOD promotes survival of circulating breast cancer cells and increases their resistance to doxorubicin. Oncotarget 7(31):50239–50257
14. Luo KQ, Yu VC, Pu Y, Chang DC (2001) Application of the fluorescence resonance energy transfer method for studying the dynamics of caspase-3 activation during UV-induced apoptosis in living HeLa cells. Biochem Biophys Res Commun 283(5):1054–1060
15. Anand P, Fu A, Teoh SH, Luo KQ (2015) Application of a fluorescence resonance energy transfer (FRET)-based biosensor for detection of drug-induced apoptosis in a 3D breast tumor model. Biotechnol Bioeng 112(8):1673–1682
16. Regmi S, Fu A, Luo KQ (2017) High shear stresses under exercise condition destroy circulating tumor cells in a microfluidic system. Sci Rep 7:39975
17. Ma S, Fu A, Chiew GGY, Luo KQ (2017) Hemodynamic shear stress stimulates migration and extravasation of tumor cells by elevating cellular oxidative level. Cancer Lett 388:239–248
18. Biganzoli L, Minisini A, Aapro M, Di Leo A (2004) Chemotherapy for metastatic breast cancer. Curr Opin Obstet Gynecol 16(1):37–41
19. Cortés-Funes H, Coronado C (2007) Role of anthracyclines in the era of targeted therapy. Cardiovasc Toxicol 7(2):56–60
20. Dillman RO, Barth NM, VanderMolen LA, Allen K, Beutel LD, Chico S (2005) High-dose chemotherapy and autologous stem cell rescue for metastatic breast cancer: superior survival for tandem compared with single transplants. Am J Clin Oncol 28(3):281–288
21. Thorn CF, Oshiro C, Marsh S, Hernandez-Boussard T, McLeod H, Klein TE, Altman RB (2011) Doxorubicin pathways: pharmacodynamics and adverse effects. Pharmacogenet Genom 21(7):440
22. Nitiss JL (2002) DNA topoisomerases in cancer chemotherapy: using enzymes to generate selective DNA damage. Curr Opin Investig Drugs 3(10):1512–1516
23. Bidwell GL III, Raucher D (2006) Enhancing the antiproliferative effect of topoisomerase II inhibitors using a polypeptide inhibitor of c-Myc. Biochem Pharmacol 71(3):248–256
24. Synowiec E, Hoser G, Bialkowska-Warzecha J, Pawlowska E, Skorski T, Blasiak J (2015) Doxorubicin differentially induces apoptosis, expression of mitochondrial apoptosis-related genes, and mitochondrial potential in BCR-ABL1-expressing cells sensitive and resistant to imatinib. BioMed Res Int 2015(673512):9
25. Malek AM, Alper SL, Izumo S (1999) Hemodynamic shear stress and its role in atherosclerosis. JAMA 282(21):2035–2042
26. Barnes JM, Nauseef JT, Henry MD (2012) Resistance to fluid shear stress is a conserved biophysical property of malignant cells. PLoS ONE 7(12):e50973
27. Chin LK, Yu JQ, Fu Y, Yu T, Liu AQ, Luo KQ (2011) Production of reactive oxygen species in endothelial cells under different pulsatile shear stresses and glucose concentrations. Lab Chip 11(11):1856–1863
28. Ye MX, Zhao YL, Li Y, Miao Q, Li ZK, Ren XL, Song LQ, Yin H, Zhang J (2012) Curcumin reverses cis-platin resistance and promotes human lung adenocarcinoma A549/DDP cell apoptosis through HIF-1alpha and caspase-3 mechanisms. Phytomedicine 19(8–9):779–787
29. Miao Q, Bi LL, Li X, Miao S, Zhang J, Zhang S, Yang Q, Xie YH, Zhang J, Wang SW (2013) Anticancer effects of bufalin on human hepatocellular carcinoma HepG2 cells: roles of apoptosis and autophagy. Int J Mol Sci 14(1):1370–1382